# The Nonlinearity of Regulation in Biological Networks

**David Murrugarra** ( murrugarra@uky.edu )
University of Kentucky
**Santosh Manicka**
Tufts University
**Kathleen Johnson**
University of Kentucky https://orcid.org/0000-0003-0432-0362
**Michael Levin**
Tufts University

**Article**

**Keywords:** Nonlinearity, Biological networks, Boolean decomposition

**Posted Date:** July 28th, 2022

**DOI:** https://doi.org/10.21203/rs.3.rs-1832497/v1

# THE NONLINEARITY OF REGULATION IN BIOLOGICAL NETWORKS

**Santosh Manicka**[*] Tufts University
**Kathleen Johnson*** University of Kentucky
**Michael Levin** Tufts University
**David Murrugarra**[†] University of Kentucky

June 30, 2022

**ABSTRACT**

Nonlinearity is a characteristic of complex biological regulatory networks that has implications ranging from therapy to control. To better understand its nature, we analyzed a suite of published Boolean network models, containing a variety of complex nonlinear interactions, using a probabilistic generalization of Boolean logic that George Boole himself had proposed. The continuous-nature of this formulation made the models amenable to Taylor decomposition that revealed their distinct layers of nonlinearity. A comparison of the resulting series of approximations of the models with the corresponding sets of randomized ensembles showed that the biological networks are on average relatively less nonlinear, suggesting that they may have been optimized for linearity by natural selection for the purpose of controllability. A further categorical analysis of the biological models revealed that the nonlinearity of cancer and disease networks could not only be sometimes higher than expected but are also relatively more variable, suggesting that the agents of disease may leverage the heterogeneity of regulatory nonlinearity to their advantage.

***Keywords*** Nonlinearity · Biological networks · Boolean decomposition

## 1 Introduction

How nonlinear are biological regulatory networks? That is, to what extent do the biochemical components of these networks non-independently interact in influencing downstream processes (Fig 1). Research on this front has hitherto focused on the various manifestations of nonlinearity in the dynamics of biological systems, such as chaos, bifurcation, multistability, synchronization, patterning, dissipation, etc.[1], but a characterization of nonlinearity in the underlying systems that give rise to those phenomena is lacking. A more complete understanding of biological nonlinearity would have theoretical implications ranging from canalization to control [2, 3] and practical implications for biomedical therapy, synthetic biology, etc. [1, 4]. A good example of this concerns the mapping between molecular or genetic information and the resulting system-level anatomical structure and function of an organism. Advances in regenerative medicine and synthetic morphology require rational control of physiological and anatomical outcomes [5], but progress in genetics and molecular biology produce methods and knowledge targeting the lowest-level cellular hardware. There is no one-to-one mapping from genetic information to tissue- and organ-level structure; similarly, ion channels open and close post-translationally, driving physiological dynamics that are not readily inferred from proteomic or transcriptomic data. System-level properties in biology are often highly emergent, with gene-regulatory or bioelectric circuit dynamics connecting initial state information and transition rules to large-scale structure and function. Thus, the difficult inverse problem [6] of inferring outcomes and desirable interventions across scales of biology illustrates some of the fundamental questions about the directness or nonlinearity of encodings of information, as well as the importance of this question for practical advances in biomedicine and bioengineering that exploit the plasticity and robustness of cellular collectives. Many deep questions remain about the potential limitations and best strategies to bridge scales

[*] Author contributions: S.M. and D.M. conceived the study; S.M. and K.J. designed code; K.J. performed research and simulations; S.M., K.J., and D.M. analyzed data; M.L. helped bridge the theory to biology. All authors helped in the writing of the manuscript. All authors approved the final version of the manuscript.
The authors have declared that no competing interests exist.
*S.M. contributed equally to this work with K.J.
†To whom correspondence should be addressed. E-mail: murrugarra@uky.edu

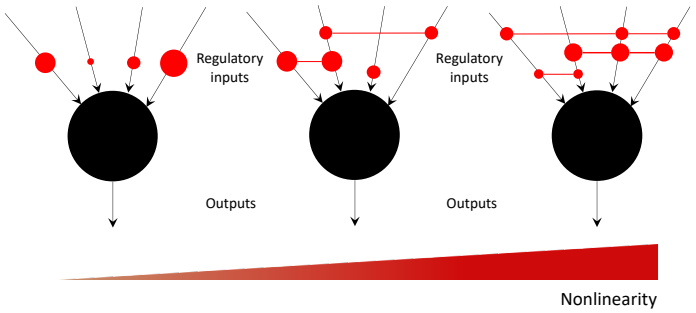


Figure 1: An illustration of the concept of regulatory nonlinearity. Each black circle represents a generic biochemical component such as a gene, transcription factor, enzyme, etc., regulated by a set of inputs (also biochemical components) and generates a generic output such as concentration level, strength, etc. Non-zero interactions among the inputs are represented by red circles connected by red lines, with the total number of possible interactions for a node with $k$ inputs equal to $\sum_{l=1}^{k} \binom{k}{l}$. The size of the red circles and the width of the connecting lines represents the weight of the interactions. Independent inputs are represented by unconnected red circles. The degree of nonlinearity thus increases from left to right, as the numbers and the strengths of the regulatory interactions increase. One could also visualize these local interactions in a broader network-context as "hypergraphs" [15].

for prediction and control in developmental, evolutionary, and cell biology. To that end, we introduce here a formal characterization of the nonlinearity of models of biological regulatory networks, such as those often used to describe relationships between regulatory genes. Specifically, we consider a class of discrete models of biological regulatory systems called "Boolean models" that are known for their relative simplicity and tractability compared to continuous ordinary differential equation-based (ODE) models [7].

A Boolean network is a discrete network model characterized by the following features. Each node in a Boolean network can only be in one of two states, ON or OFF, which represents the expression or activity of that node. The state of a node depends on the states of other input nodes which are represented as a Boolean rule of these input nodes. Many of the available Boolean network models were created via literature search of the regulatory mechanisms and subsequently validated via experiments [8]. Some of the publicly available models were generated via network inference methods from time course data [2].

Previous studies have found that certain characteristic features of the biological Boolean models, such as the mean in-degree, output bias, sensitivity and canalization, tend to assume an optimal range of values that support optimal function [9, 10]. Here we study a new but generic feature of complex systems, namely, nonlinearity. To characterize the nonlinearity of Boolean networks we formalize an approach to generalizing Boolean logic by casting it as a form of probability, which was originally proposed by George Boole himself [11]. We leverage the continuous nature of these polynomials to decompose a Boolean function using Taylor-series and reveal its distinct layers of nonlinearity (Fig 2). Various other methods, both discrete and continuous, of decomposing Boolean functions exist, such as Reed-Muller, Walsh spectrum, Fourier and discrete Taylor [12, 13, 14]. Our continuous Taylor decomposition method is distinct in that it offers a clear and systematic way to characterize nonlinearity.

By characterizing the nonlinearity of networks in this way, we answer the following questions: 1) how well could biological Boolean models be approximated, that is, faithfully represented with only partial information containing lower levels of nonlinearity relative to that of the original?; 2) is there an optimal level of nonlinearity, characterized by maximum approximability, that these models may have been selected for by evolution?; and 3) do different classes of biological networks show characteristically different optimal levels of nonlinearity? To answer these questions, we first approximate the biological models by systematically composing the various nonlinear layers resulting in a sequence of model-approximations with increasing levels of nonlinearity. We then estimate the accuracy of these approximations by comparing the outputs of their simulations with that of the original unapproximated model. We then construct an appropriate random ensemble for each biological model and compare their mean accuracies for fixed levels of approximation. The main idea is that a biological model that is more approximable than expected for a particular level of nonlinearity would mean that the network may have been optimized for that level nonlinearity. Finally, we classify the biological networks into various categories and compare their approximabilities to identify any category-dependent effects.

## Methods

### Probabilistic generalization of Boolean logic

Here we provide a continuous-variable formulation of a Boolean function by casting Boolean values as probabilities, thus transforming it into a pseudo-Boolean function [16]. Consider random variables $X_i : \{0,1\} \to [0,1]$, $i = 1, \ldots, n$, with Bernoulli distributions. That is, $p_i = Pr(X_i = 1) = 1 - Pr(X_i = 0) = 1 - q_i$, for $i = 1, \ldots, n$. Let $X = X_1 \times \cdots \times X_n$ be the product of random variables and $f : X \to \{0,1\}$ a Boolean function. Let $R_0^f = \{x \in X : f(x) = 0\}$ and $R_1^f = \{x \in X : f(x) = 1\}$. Note that $X$ is a disjoint union of $R_0^f$ and $R_1^f$. Then, $Pr(f = 1) = Pr(R_1^f) = \sum_{x \in R_1^f} Pr(x) = \sum_{x \in R_1^f} \prod_{i=1}^n \hat{p}_i$ where $\hat{p}_i = p_i$ if $x_i = 1$ and $\hat{p}_i = 1 - p_i$ if $x_i = 0$. Let $\hat{f}(p_1, \ldots, p_n) = \sum_{x \in R_1^f} \prod_{i=1}^n \hat{p}_i$. Thus, $\hat{f} : [0,1]^n \to [0,1]$ is a continuous-variable function. The following theorem shows that $\hat{f}$ is a generalization of $f$ in the sense that $\hat{f}(x) = f(x)$ for all $x \in \{0,1\}^n$; proof is provided in SI Appendix.

**Theorem 1.1.** *For discrete values of $x_i \in \{0,1\}$, $i = 1, \ldots, n$, we have $\hat{f}(x_1, \ldots, x_n) = f(x_1, \ldots, x_n)$.*

**Corollary 1.2.** *If $p_i = 1/2$ for all $i = 1, \ldots, n$, then $\hat{f}(p_1, \ldots, p_n)$ is the output bias of $f$.*

**Example 1.3.** *Consider the AND, OR, XOR, and NOT Boolean functions given in Table 1. The continuous-variable generalization of $f_1$, $f_2$, $f_3$, and $f_4$ are: $\hat{f}_1 = x_1x_2$, $\hat{f}_2 = (1 - x_1)x_2 + x_1(1 - x_2) + x_1x_2 = x_1 + x_2 - x_1x_2$, $\hat{f}_3 = (1 - x_1)x_2 + x_1(1 - x_2) = x_1 + x_2 - 2x_1x_2$, and $\hat{f}_4 = 1 - x$.*

Note that the above expressions have previously been derived via other (not probability-based) means [14].

| $x_1$ | $x_2$ | $f_1$ | $f_2$ | $f_3$ |
|---|---|---|---|---|
| 0 | 0 | 0 | 0 | 0 |
| 0 | 1 | 0 | 1 | 1 |
| 1 | 0 | 0 | 1 | 1 |
| 1 | 1 | 1 | 1 | 0 |

| $x$ | $f_4$ |
|---|---|
| 0 | 1 |
| 1 | 0 |

Table 1: Truth tables of basic Boolean functions.

### Taylor Decomposition of Boolean functions

Since $\hat{f}$ is a continuous-variable function, we can calculate its Taylor expansion. And since $\hat{f}$ is a square-free polynomial, its Taylor expansion is finite and simplified (any term containing multiple derivatives of the same variable is zeroed out), as described in Proposition 1.4 using the standard multi-index notation. Let $\alpha = (\alpha_1, \ldots, \alpha_n)$ where $\alpha_i \in \{0,1\}$. We define $\mid \alpha \mid = \alpha_1 + \cdots + \alpha_n$, $x^\alpha = x_1^{\alpha_1} x_2^{\alpha_2} \cdots x_n^{\alpha_n}$, and $\partial^\alpha f = \partial_1^{\alpha_1} \partial_2^{\alpha_2} \cdots \partial_n^{\alpha_n} f = \frac{\partial^{|\alpha|} f}{\partial_1^{\alpha_1} \partial_2^{\alpha_2} \cdots \partial_n^{\alpha_n}}$.

**Proposition 1.4.** *For $p \in [0,1]^n$, we have*

$$\hat{f}(x) = \hat{f}(p) + \sum_{1 < |\alpha| \leq n} \partial^\alpha \hat{f}(p)(x - p)^\alpha. \tag{1}$$

Note that $\hat{f}(p)$ in Equation 1 is the output bias of $f$ as was seen in Corollary 1.2. A natural choice for $p$ is $p = (1/2, \ldots, 1/2)$ as it represents an unbiased selection for each variable and it also gives the output bias of the function. Such unbiased choices are not available for the discrete case. Our continuous formulation thus offers such unique advantages over the discrete Taylor decomposition, as it's a natural generalization of the latter. The Taylor decomposition can be used to approximate a Boolean function by considering a subset of the terms. For example, a linear approximation consists of terms only up to $|\alpha| \leq 1$, a bilinear approximation up to $|\alpha| \leq 2$, etc., up until $|\alpha| \leq n$ where it ceases to be an approximation and provides an exact decomposition of $\hat{f}$. A visual illustration is provided in Figure 2. The approximation order of a Boolean *network* could therefore vary between its minimum and maximum in-degrees (number of inputs per node).

| Derivative | $f_1$ | $f_2$ | $f_3$ |
|---|---|---|---|
| $\partial_1$ | 0.5 | 0.5 | 0 |
| $\partial_2$ | 0.5 | 0.5 | 0 |
| $\partial_1\partial_2$ | 1 | -1 | -2 |

| Derivative | $f_4$ |
|---|---|
| $\partial_1$ | -1 |

Table 2: Values of partial the derivatives in the Taylor decompositions of the generalizations of basic Boolean functions.

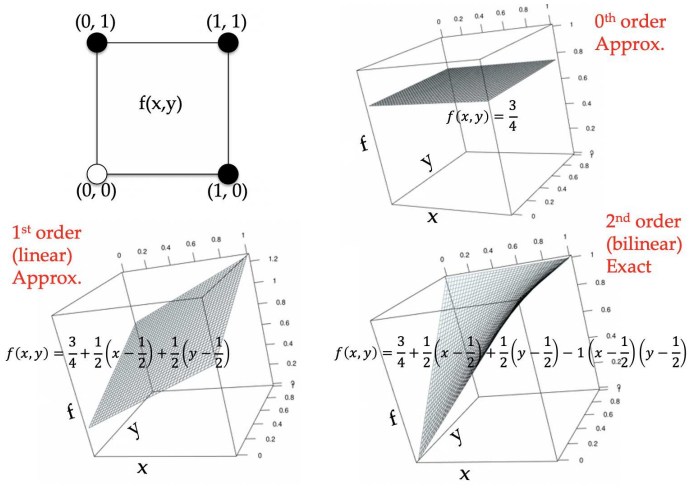


Figure 2: The various approximations of a Boolean function according to the amount of nonlinearity retained. The logical OR function is represented as a 2D hypercube (top left) with the coordinate values representing input combinations and the color of the circles representing the corresponding outputs (white=0, black=1) and is approximated using Taylor decomposition as the $0^{th}$ order approximation (top right) showing only the first term, the mean output bias; the $1^{st}$ order approximation (bottom left) including the linear terms; and finally the $2^{nd}$ order exact form (bottom right) including all the terms.

**Example 1.5.** *Consider the continuous generalizations of the AND, OR, XOR and NOT functions given in Example 1.3 The corresponding Taylor expansions using Equation 1 and using the derivatives shown in Table 2 with* $p = (1/2, 1/2)$ *are:* $\hat{f}_1 = 0.25 + 0.5(x_1 - 0.5) + 0.5(x_2 - 0.5) + (x_1 - 0.5)(x_2 - 0.5)$, $\hat{f}_2 = 0.75 + 0.5(x_1 - 0.5) + 0.5(x_2 - 0.5) - (x_1 - 0.5)(x_2 - 0.5)$, $\hat{f}_3 = 0.5 - 2(x_1 - 0.5)(x_2 - 0.5)$, *and* $\hat{f}_4 = 0.5 - (x - 0.5) = 1 - x$.

Note that $\hat{f}_1(1/2, 1/2) = 0.25$, $\hat{f}_2(1/2, 1/2) = 0.75$, $\hat{f}_3(1/2, 1/2) = 0.5$, and $\hat{f}_4(1/2) = 0.5$ in the above equations are the output biases of the AND, OR, XOR, and NOT functions respectively. Also note that both the AND and OR functions contain the linear and the second order terms in their Taylor decomposition while the XOR function only contains the second order term. This difference is because both the AND and OR functions are monotone while XOR is not since it requires both inputs to be known.

### Approximability of a model

We considered a suite of Boolean network models of biochemical regulation from two sources, namely the *cell collective* [8] and reference [2]. This suite consists of 137 networks with the number of nodes ranging from 5 to 321. The mean in-degree of these models ranges from 1.1818 to 4.9375 with the variances ranging between $0.1636$ and $9.2941$, while the mean output bias is limited to the range [0.1625,0.65625] with the variances between $0.0070$ and $0.0933$. For each biological model we generated an associated ensemble of 100 randomized models, where the connectivity and the output bias of the nodes of the original model were preserved and the logic rules were randomly chosen under the above constraints. This approach helps avoid confounding the causes of any observed effects with network structure or output bias, thereby narrowing the focus on the role of nonlinearity. We applied the Taylor decomposition to both the biological models and the associated ensembles and computed all possible nonlinear approximations. Both the biological models and the associated random ensembles were then simulated using a set of 1000 randomly chosen initial states iterated through 500 update steps for all orders of approximation; the same initial conditions were used for a given biological model and the associated random ensemble. The states of the variables were restricted to the interval [0,1] at every step in the simulations. We then computed the mean approximation error (MAE) of each model as the percentage mean squared error (MSE) between the exact Boolean states and the approximated probabilistic states at the end of the simulations; for the random ensembles we computed a single average MAE. Finally, we computed the "approximability" of each biological model as the difference between the MAE of the associated random ensemble and its MAE. Per these definitions, the MAE can range between 0.0 and 100.0, while the approximability can range between -100.0 and 100.0.

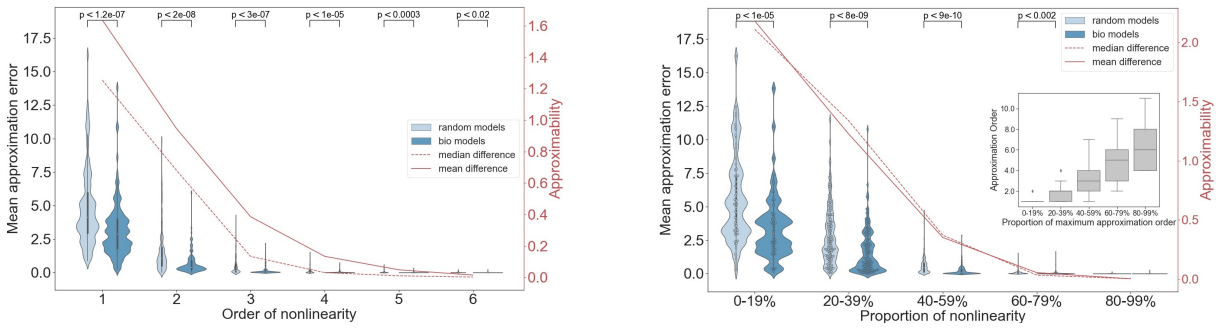


(a) (b)

Figure 3: Biological models are more approximable for various degrees of nonlinearity compared to a reference random ensemble. (a) Comparison with respect to the absolute approximation order; MAE values for orders above 6 are negligible and thus not shown. (b) Comparison with respect to the normalized approximation order (ratio of the actual approximation order to the maximum), where the maximum order of approximation for a model is equal to its max in-degree. The inset shows the spread of the absolute approximation orders for every proportion bucket. Every point in the light blue plots represents the average MAE of an ensemble of 100 random networks associated with each biological model. The p-values indicate the statistical significance of the difference in means between the set of random ensembles and the biological models for a given order of nonlinearity. Statistical analysis by Welch's unequal variances t-test.

### Classification of biological models

To identify any differences among the approximabilities of different types of biological networks we sought to classify them. Since there are multiple ways to classify biological networks, we chose two classifications so that: 1) they are as orthogonal as possible to each other; and 2) each classification has an appropriate number of (neither too few nor too many) categories. Classification 1 (C1) follows the "pathway ontology" (PW) [17] where the networks are grouped into five categories (Figure 4(a)), namely biochemical ($n = 13$), signaling ($n = 22$), disease ($n = 55$), metabolic ($n = 14$) and regulatory ($n = 33$). According the definitions used in the PW ontology, a "signaling" network comprises mainly of extracellular signal transduction components such as growth factors, kinases, etc. A "regulatory" network, on the other hand, comprises intracellular transcriptional components such as genes, transcription factors, etc. The term "biochemical" here refers to networks that comprises a mix of signaling and regulatory components. "Metabolic" networks consist of components involved in the synthesis and conversion of biomolecules such as enzymes and lipids. Finally, "disease" networks consist of components involved in diseases such as cancer, anemia, pathogenic ailments and disorders such as cell cycle malfunction. Classification 2 was suggested by in-house expertise, where the networks are grouped into four categories (Figure 4(b)), namely metazoan ($n = 85$), cancer ($n = 24$), primitive ($n = 19$) and plants ($n = 9$). The "metazonan" category refers to multicellular organisms and "primitive" refers to unicellular organisms. A given model could naturally belong in multiple categories within a classification but is assigned a unique category for the purpose of simplicity; we chose the categories according to the emphasis laid in the abstracts of the corresponding publications. More details are provided in the SI Appendix (Table S1).

## Results and Discussion

### Biological networks are less nonlinear than expected by chance

We found that the biological models are relatively more approximable for various degrees of nonlinearity when compared to a reference ensemble (Figure 3). The contrast is most prominent in the linear regime where the biological models are about 2% more approximable ($p < 10^{-5}$) compared to their random counterparts. This suggests that the biological regulatory networks may have been optimized (presumably by evolution) for linearity in the nonlinearity of the Boolean rules, given that the reference ensemble preserves the network structure and the output biases of the corresponding biological models. This has implications not only for the feasibility of biomedical approaches to control emergent somatic complexity or guided self-assembly of novel forms [18], but also for models of anatomical homeostasis and evolvability: linearity implies easier control of its own complex processes by any biological system, and more efficient credit assignment during evolution.

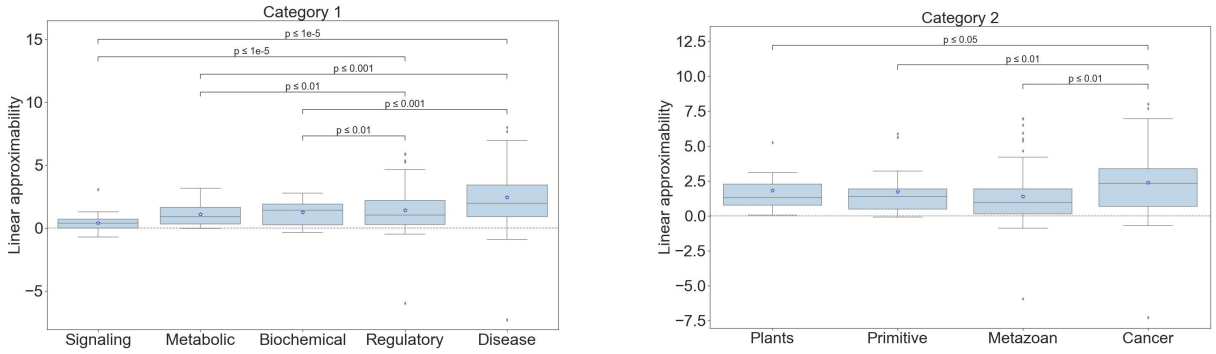


(a) (b)

Figure 4: The linear approximabilities of various categories of biological models. (a) Classification 1 (C1); (b) Classification 2 (C2). The categories in either classification are displayed in increasing order of variance. Each box represents the distribution of the linear approximabilities of the corresponding category. The p-values indicate the statistical significance of the difference in the variance between pairs of categories; only the p-values of significantly different pairs are shown. Statistical analysis by F-test of equality of variances.

**The approximability of a biological network depends on its class, with the cancer family displaying the most variability**

Even though the nonlinearity of biological networks is less than expected on average, individual and category-dependent variations were observed. In the following, we focus on the approximability corresponding to the linear order ("linear approximability") of biological networks since it's maximized at the linear regime (Figure 3). First, there are a few networks that are more nonlinear than expected as evidenced by the negative linear approximability (Fig 4). Second, the disease networks in C1 and the cancer networks in C2 are the ones with the most linear approximability (high positive values). In other words, the cancer or disease pathways tend to be more optimized for linearity compared to the other categories. This makes sense since a more linear pathway is more amenable to control, which presumably works in favour of the agents of disease. Moreover, the disease and cancer networks also display the highest variability in their linear approximability compared to other categories ($p < 0.05$ in all comparisons), with the corresponding values extending into the negative regime as well, that is they are sometimes more nonlinear than expected. Note that about 56% of the disease category comprises of non-cancer networks (31/55), which suggests that the effect is not significantly biased by cancer networks. Taken together, these observations suggest that regulatory nonlinearity may offer an effective "entry point" to the agents of disease by virtue of its natural heterogeneity that they could leverage to their advantage perhaps as a means to evade treatment since there's no single level of nonlinearity to target. This heterogeneity may also have a connection to one of the hallmarks of cancer, namely genetic heterogeneity [19] where the cancerous cells within an individual display heterogeneous gene expression compared to the homogeneous expression in the healthy cells. In the case of nonlinearity, the heterogeneity manifests at the population level, raising the question of whether it may also be observed at the level of single cells within an individual. In other words, could the heterogeneity of nonlinearity be yet another hallmark of cancer?

**The shape of the Taylor spectrum explains the extreme opposite characters of linear approximability of a pair of cancer models**

Why are some models more linearly approximable and others less? The answer lies in the organization of the corresponding Taylor decompositions, as described above. To illustrate this in detail, we compared the Taylor decompositions of the least and the most linearly approximable models in our dataset (the two most extreme outliers in Fig 4). Those models respectively are the following: a model describing the role of mutations in the regulation of metastasis in lung cancer [20] and henceforth referred to as the 'Metastasis' model ; and a model describing the role of the protein p53 in the regulation of cell-cycle arrest in breast cancer [21] and henceforth referred to as the 'P53' model. Both P53 and Metastasis are models of cancer, as may be expected from Fig 4. P53 has a linear approximability of about 8.02 and it consists of 16 nodes with a mean in-degree of $3.8\pm2.4$ and a mean output bias of $0.38\pm0.14$, while Metastasis has a linear approximability of about -7.28 and it consists of 32 nodes with a mean in-degree of $4.9\pm2.5$ and a mean output bias of $0.27\pm0.26$. Thus, while P53 is smaller and sparser than Metastasis, its nodes exhibit more output-uncertainty compared to Metastasis. According to the mean field theory of random Boolean networks [22], the opposite characters of the mean in-degree and the output bias of these models means that

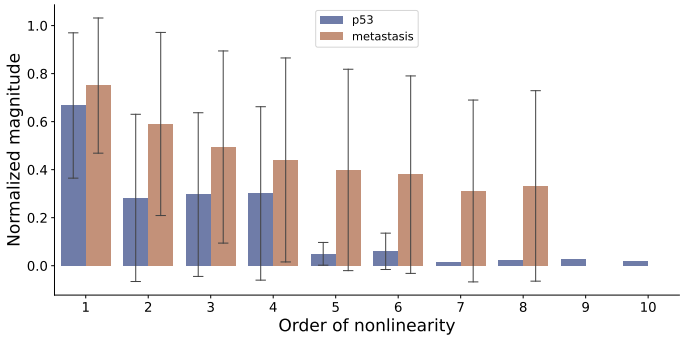


Figure 5: A comparison of the spectrums of the magnitudes of nonlinearity of the models corresponding to the two extreme cases of approximability. The bars represent the mean absolute value of all the Taylor derivatives of the corresponding order, averaged over all the nodes of the corresponding model containing those terms. The maximum orders (in-degrees) of P53 and Metastasis are respectively 10 and 8. and To compare the derivatives from different models they were normalized with respect to the maximum possible absolute value of a Taylor derivative of order $|\alpha|$ (Equation 1) of a Boolean function with output bias $p$, given by $(\min(p, 0.5) - \max(p - 0.5, 0))2^{|\alpha|}$ (proof provided in the SI Appendix). The error bars represent the standard deviation and not the confidence intervals of the means since they are not estimates. The errors appear large whenever the corresponding distribution of the magnitudes are bimodal with many values clustered close to 0.

their dynamical behaviors could be expected to be similar (although with the caution that the theory was originally developed for infinite-sized and homogeneously connected networks, which is not the case here). However, we know that their linear approximabilities, which is another expression of dynamical behavior, are opposites. One explanation for this discrepancy lies in the distinct apportioning of nonlinearity in their respective Taylor decompositions (Fig 5). Specifically, while the magnitude of nonlinearity, defined as the mean absolute value of the Taylor derivatives for a given order and normalized appropriately (see text of Fig 5), tends to be clustered around the linear order for P53, they are relatively more spread out for Metastasis. Moreover, while the magnitude of the linear order for P53 is more than twice as large the next largest magnitude at lower orders the corresponding ratios for Metastasis are relatively smaller, thus explaining why P53 is more linearly approximable than Metastasis. This result is consistent with predictions based on a model of scaling of cellular control policies [23]. A more controllable (linear) network (P53) is optimal for cooperation with other cells towards collective (normal morphogenetic) goals. In contrast, a cell defecting from the collective and reverting to a more unicellular lifestyle (Metastasis) should exhibit a less predictable, controllable network due to pressures from parasites and competitors that independent unicellular organisms face. Methods for calculating controllability (e.g., linearity) are an important addition to recent efforts to solve the conundrum of interpretability of information structures in contexts ranging from machine learning to evolutionary developmental biology [24, 25, 26].

**Broader implications**

This paper introduces the concept of regulatory nonlinearity as a new measure of characterization for Boolean networks. There are several other related characterizations of Boolean networks such as canalization [27], effective connectivity [10], symmetry [28] and controllability [29]. It has been previously reported that the levels of canalization (a measure of the extent to which fewer inputs influence the outputs of a Boolean function) and the mean effective connectivity (a measure of collective canalization) are high in biological networks [2, 10]. It has also been found that biological networks need few inputs to reprogram [30] and are relatively easier to control [3]. Our formulation of regulatory nonlinearity is related to these other measures in that more linearity implies more apportioning of influence to individual inputs rather than collective sets of inputs (Figure 5). Hence, we hypothesize that regulatory nonlinearity may serve the purpose of controllability and epigenetic stability [31]. Our results further moot the possibility that regulatory nonlinearity may be a factor underlying more powerful dynamical phenomena such as memory [32] and computation, defined as the capacity for adaptive information-processing [33]. Even though there's increasing consensus that biological systems contain memory and perform computation, clarity is lacking as to what features of those systems enable it and what general principles underlie it [33, 34]. Our framework of regulatory nonlinearity offers an approach to answering these questions. For example, one could consider a known dynamical model with a capacity for memory [32] or universal computation such as the elementary cellular automaton (ECA) driven by rule 110 [35] and ask if there are unique properties of its Taylor spectrum that confer their respective capabilities. Present approaches to answering this question typically consists of characterization of the dynamical behavior and not the rules [36, 37, 32]. A characterization of the rules especially makes sense for ECA [38] since the structure is always the same (lattice) and

the only feature that distinguishes one ECA from the other is the rule. Looking at such questions from an even broader perspective it becomes evident that they are only instances of the ultimate puzzle of complex systems, namely what connects the structure and the function of a system. Even though recent work has attempted to answer this question from the perspective of the rules or dynamical laws that govern the system [39, 10, 38], more tools are needed [40]. In that regard, our framework of regulatory nonlinearity could be a novel addition to this burgeoning toolkit in that it could also be applied to continuous models of biological networks such as those based on differential equations.

### Limitations

The main limitation of our formulation of approximability is that the approximation accuracy will necessarily increase with higher orders of approximation for arbitrary Boolean networks (the highest order of approximation is exact). However, this does not affect the falsifiability of our framework since it's possible to construct networks, say with XOR-like functions, that are less linearly approximable than the associated ensembles. The Metastasis model is another example in that regard (Figure 5). Furthermore, the notion of nonlinearity is limited to the local level of the Boolean rules in our framework, whereas its possible to conceive network-level measures of nonlinearity where the role of the network structure is included. Lastly, our conclusions about the linearity of biological regulatory networks may be a reflection of a hidden bias built in the inference methods that produced the models in the first place. We leave it to future work to explore these realms.

## References


[1] Tomasz Kapitaniak and Sajad Jafari. Nonlinear effects in life sciences, 2018.

[2] Claus Kadelka, Taras-Michael Butrie, Evan Hilton, Jack Kinseth, and Haris Serdarevic. A meta-analysis of boolean network models reveals design principles of gene regulatory networks. *arXiv preprint arXiv:2009.01216*, 2020.

[3] Enrico Borriello and Bryan C. Daniels. The basis of easy controllability in boolean networks. *Nature Communications*, 12(5227), 2021.

[4] Ruud Stoof and Ángel Goñi-Moreno. Modelling co-translational dimerization for programmable nonlinearity in synthetic biology. *Journal of the Royal Society Interface*, 17(172):20200561, 2020.

[5] Giovanni Pezzulo and Michael Levin. Top-down models in biology: explanation and control of complex living systems above the molecular level. *Journal of The Royal Society Interface*, 13(124):20160555, 2016.

[6] Daniel Lobo, Mauricio Solano, George A Bubenik, and Michael Levin. A linear-encoding model explains the variability of the target morphology in regeneration. *Journal of The Royal Society Interface*, 11(92):20130918, 2014.

[7] Assieh Saadatpour and Réka Albert. A comparative study of qualitative and quantitative dynamic models of biological regulatory networks. *EPJ Nonlinear Biomedical Physics*, 4(1):1–13, 2016.

[8] Tomáš Helikar, B Kowal, and JA Rogers. A cell simulator platform: the cell collective. *Clinical Pharmacology & Therapeutics*, 93(5):393–395, 2013.

[9] Bryan C Daniels, Hyunju Kim, Douglas Moore, Siyu Zhou, Harrison B Smith, Bradley Karas, Stuart A Kauffman, and Sara I Walker. Criticality distinguishes the ensemble of biological regulatory networks. *Physical review letters*, 121(13):138102, 2018.

[10] Santosh Manicka, Manuel Marques-Pita, and Luis M Rocha. Effective connectivity determines the critical dynamics of biochemical networks. *Journal of the Royal Society Interface*, 19(186):20210659, 2022.

[11] George Boole. Collected logical works, vol. i. *Studies in Logic and Probability, R. Rhees (ed.), Open Court Publ. Co., LaSalle, Ill*, 1952.

[12] Ryan O'Donnell. *Analysis of boolean functions*. Cambridge University Press, 2014.

[13] SN Yanushkevich and VP Shmerko. Taylor expansion of logic functions: From conventional to nanoscale design. In *Int. TICSP Workshop on Spectral Methods and Multirate Signal Processing*. Citeseer, 2004.

[14] Melanie Grieb, Andre Burkovski, J Eric Sträng, Johann M Kraus, Alexander Groß, Günther Palm, Michael Kühl, and Hans A Kestler. Predicting variabilities in cardiac gene expression with a boolean network incorporating uncertainty. *PloS one*, 10(7):e0131832, 2015.

[15] Federico Battiston, Enrico Amico, Alain Barrat, Ginestra Bianconi, Guilherme Ferraz de Arruda, Benedetta Franceschiello, Iacopo Iacopini, Sonia Kéfi, Vito Latora, Yamir Moreno, et al. The physics of higher-order interactions in complex systems. *Nature Physics*, 17(10):1093–1098, 2021.

[16] William H Press, Brian P Flannery, Saul A Teukolsky, and William T Vetterling. Numeric recipes in c: the art of scientific computing. *Camb. Univ. Press Camb*, 1992.

[17] Victoria Petri, Pushkala Jayaraman, Marek Tutaj, G Thomas Hayman, Jennifer R Smith, Jeff De Pons, Stanley JF Laulederkind, Timothy F Lowry, Rajni Nigam, Shur-Jen Wang, et al. The pathway ontology–updates and applications. *Journal of biomedical semantics*, 5(1):1–12, 2014.

[18] Mo R Ebrahimkhani and Michael Levin. Synthetic living machines: A new window on life. *Iscience*, page 102505, 2021.

[19] Douglas Hanahan and Robert A Weinberg. Hallmarks of cancer: the next generation. *cell*, 144(5):646–674, 2011.

[20] David PA Cohen, Loredana Martignetti, Sylvie Robine, Emmanuel Barillot, Andrei Zinovyev, and Laurence Calzone. Mathematical modelling of molecular pathways enabling tumour cell invasion and migration. *PLoS computational biology*, 11(11):e1004571, 2015.

[21] Minsoo Choi, Jue Shi, Sung Hoon Jung, Xi Chen, and Kwang-Hyun Cho. Attractor landscape analysis reveals feedback loops in the p53 network that control the cellular response to dna damage. *Science signaling*, 5(251):ra83–ra83, 2012.

[22] Bernard Derrida and Yves Pomeau. Random networks of automata: a simple annealed approximation. *EPL (Europhysics Letters)*, 1(2):45, 1986.

[23] Michael Levin. Bioelectrical approaches to cancer as a problem of the scaling of the cellular self. *Progress in biophysics and molecular biology*, 165:102–113, 2021.

[24] Pantelis Linardatos, Vasilis Papastefanopoulos, and Sotiris Kotsiantis. Explainable ai: A review of machine learning interpretability methods. *Entropy*, 23(1):18, 2020.

[25] Santosh Manicka and Michael Levin. Minimal developmental computation: A causal network approach to understand morphogenetic pattern formation. *Entropy*, 24(1):107, 2022.

[26] Richard A Watson, Michael Levin, and Christopher L Buckley. Design for an individual: connectionist approaches to the evolutionary transitions in individuality. *Frontiers in Ecology and Evolution*, page 64, 2022.

[27] Stuart Kauffman. The large scale structure and dynamics of gene control circuits: an ensemble approach. *Journal of Theoretical Biology*, 44(1):167–190, 1974.

[28] CJ Olson Reichhardt and Kevin E Bassler. Canalization and symmetry in boolean models for genetic regulatory networks. *Journal of Physics A: Mathematical and Theoretical*, 40(16):4339, 2007.

[29] Alexander J Gates and Luis M Rocha. Control of complex networks requires both structure and dynamics. *Scientific reports*, 6(1):1–11, 2016.

[30] Franz-Josef Müller and Andreas Schuppert. Few inputs can reprogram biological networks. *Nature*, 478(7369):E4–E4, 2011.

[31] Andreas Wagner. Does evolutionary plasticity evolve? *Evolution*, 50(3):1008–1023, 1996.

[32] Surama Biswas, Santosh Manicka, Erik Hoel, and Michael Levin. Gene regulatory networks exhibit several kinds of memory: Quantification of memory in biological and random transcriptional networks. *Iscience*, 24(3):102131, 2021.

[33] Melanie Mitchell. Ubiquity symposium: biological computation. *Ubiquity*, 2011(February), 2011.

[34] Dominique Chu, Mikhail Prokopenko, and J Christian J Ray. Computation by natural systems, 2018.

[35] Matthew Cook et al. Universality in elementary cellular automata. *Complex systems*, 15(1):1–40, 2004.

[36] Stephen Wolfram. Statistical mechanics of cellular automata. *Reviews of modern physics*, 55(3):601, 1983.

[37] Hector Zenil and Jürgen Riedel. Asymptotic intrinsic universality and natural reprogrammability by behavioural emulation. In *Advances in Unconventional Computing*, pages 205–220. Springer, 2017.

[38] Santosh Venkatiah Sudharshan Manicka. *The role of canalization in the spreading of perturbations in Boolean networks*. PhD thesis, Indiana University, 2017.

[39] Manuel Marques-Pita and Luis M Rocha. Canalization and control in automata networks: body segmentation in drosophila melanogaster. *PloS one*, 8(3):e55946, 2013.

[40] Luis M Rocha. On the feasibility of dynamical analysis of network models of biochemical regulation. *arXiv preprint arXiv:2110.10821*, 2021.

# Supplementary Information

The nonlinearity of regulation in biological networks

Santosh Manicka, Kathleen Johnson, Michael Levin and David Murrugarra

## 1. Probabilistic generalization of Boolean logic

Here we show that $\hat{f}$ is a generalization of $f$ in the sense that $\hat{f}(x) = f(x)$ for all $x \in \{0,1\}^n$.

**Theorem 0.1.** *For discrete values of $x_i \in \{0,1\}$, $i = 1, \ldots, n$, we have*

$$\hat{f}(x_1, \ldots, x_n) = f(x_1, \ldots, x_n).$$

*Proof.* Let $z = (z_1, \ldots, z_n) \in \{0,1\}^n$. Since each $z_i$ is either 0 or 1, we have that $p_i = 1$ if $z_i = 1$ or $p_i = 0$ if $z_i = 0$ for $i = 1, \ldots, n$. We want to show that $\hat{f}(p_1, \ldots, p_n) = f(z_1, \ldots, z_n)$. Since $X = R_0^f \cup R_1^f$, we have that either $z \in R_0^f$ or $z \in R_1^f$. If $z \in R_1^f$, then $f(z) = 1$ and $Pr(z) = \prod_{i=1}^n \hat{p}_i = 1$. Moreover, for any other $x \in R_1^f$ with $x \neq z$ we have that $Pr(x) = 0$. Thus, $\hat{f}(z) = \sum_{x \in R_1^f} Pr(x) = Pr(z) = 1$. Now if $z \in R_0^f$, then $\hat{f}(z) = 0$ because $\sum_{\emptyset} = 0$. Thus, $\hat{f}(x) = f(x)$ for all $x \in \{0,1\}^n$. □

## 2. Maximum absolute value of a Taylor derivative

Here we show that $\max(|\partial^\alpha \hat{f}|) = (\min(p, 0.5) - \max(p - 0.5, 0))2^{|\alpha|}$.
We begin with the definition of the derivative given by

$$\frac{\partial \hat{f}(x_1, \ldots, x_i, \ldots, x_k)}{\partial x_i} = \lim_{h \to 0} \frac{\hat{f}(0.5, \ldots, h, \ldots, 0.5) - \hat{f}(0.5, \ldots, 0, \ldots, 0.5)}{h}$$

Since $\hat{f}$ is a pseudo-Boolean function and hence a multilinear polynomial [1], we can rewrite it by setting $h$ to 1, as a finite difference; the idea being that the derivative taken over any point on a line is the line itself:

$$\frac{\partial \hat{f}(x_1, \ldots, x_i, \ldots, x_k)}{\partial x_i} = \hat{f}(0.5, \ldots, 1, \ldots, 0.5) - \hat{f}(0.5, \ldots, 0, \ldots, 0.5)$$

Since multilinear interpolation can be formulated as weighted averaging [2], we can further rewrite it as follows (the weights are equal here since the non-binary values are all set to 0.5):

$$\frac{\partial \hat{f}(x_1, \ldots, x_i, \ldots, x_k)}{\partial x_i} = \sum_{x_1, \ldots, x_{i-1}, x_{i+1}, \ldots, x_k \in \{0,1\}} \frac{\hat{f}(x_1, \ldots, x_{i-1}, 1, x_{i+1}, \ldots, x_k) - \hat{f}(x_1, \ldots, x_{i-1}, 0, x_{i+1}, \ldots, x_k)}{2^{k-1}}$$

As can be seen, there are a total of $2^k$ terms, with half of them positively signed and half negative. This form of expression generalizes to derivatives taken over two or more variables. For example, the derivative taken over two variables, $x_i$ and $x_j$, looks as follows:

$$\frac{\partial^2 \hat{f}(\ldots, x_i, \ldots, x_j, \ldots)}{\partial x_i \partial x_j} = \sum_{x_1, \ldots, x_{i-1}, x_{i+1}, \ldots, x_k \in \{0,1\}} \sum_{x_1, \ldots, x_{j-1}, x_{j+1}, \ldots, x_k \in \{0,1\}} \left[ \frac{\hat{f}(\ldots, x_{i-1}, 1, x_{i+1}, \ldots, x_{j-1}, 1, x_{j+1}, \ldots) - \hat{f}(\ldots, x_{i-1}, 1, x_{i+1}, \ldots, x_{j-1}, 0, x_{j+1}, \ldots)}{2^{k-2}} \right] - \left[ \frac{\hat{f}(\ldots, x_{i-1}, 0, x_{i+1}, \ldots, x_{j-1}, 1, x_{j+1}, \ldots) - \hat{f}(\ldots, x_{i-1}, 0, x_{i+1}, \ldots, x_{j-1}, 0, x_{j+1}, \ldots)}{2^{k-2}} \right]$$

Following rearrangement of terms it becomes evident that this expression also contains $2^{k-1}$ positive terms and $2^{k-1}$ negative terms, with the only difference in the power of the denominator term. It can thus be concluded that any derivative $\partial^\alpha \hat{f}$ (in multi-index notation) has $2^{k-1}$ positive terms and $2^{k-1}$ negative terms.

A straightforward way to maximize the value of a derivative expressed in this form is by assigning as many instances of 1 as possible to the positive terms and as few instances of 1 as possible to the negative terms. For a Boolean function with $k$ inputs and output bias $p$, this can be accomplished by assigning $\min(2^{k-1}, p2^k)$ ones and $\max(p2^k - 2^{k-1}, 0)$ ones respectively. Therefore,

$$\begin{aligned}\max(|\partial^\alpha \hat{f}|) &= \frac{\min(2^{k-1}, p2^k) - \max(p2^k - 2^{k-1}, 0)}{2^{k-|\alpha|}} \\ &= (\min(p, 0.5) - \max(p - 0.5, 0))2^{|\alpha|}; 1 \leq |\alpha| \leq k.\end{aligned}$$

Note that this formula only applies to a specific order of nonlinearity $|\alpha|$ independent of the other orders within the same Boolean function. In actuality, there are dependencies between the various orders within a Boolean function. That is, if a Boolean function were to be constructed such that the derivative of a particular order $|\alpha_1|$ is maximized then there's no guarantee that the derivative of another order $|\alpha_2| \neq |\alpha_1|$ could be simultaneously maximized. This is one of the limitations of the normalization for which the above formula is used.

Table 1: Dataset Description

| **Pubmed** ID | **Description** | **Category 1** | **Category 2** |
|---|---|---|---|
| 1753781 | A model of tumor immunity | Disease | Cancer |
| 11082279 | A model of the growth-quiescence switch signaling pathway | Biochemical | Metazoan |
| 16464248 | A model of a typical signaling pathway where mass and signal flow occur simultaneously | Signaling | Metazoan |
| 16464248 | A model of the Tcell receptor signaling | Signaling | Metazoan |
| 16542429 | A model of the regulatory network governing the differentiation of CD4+ Tcells | Biochemical | Metazoan |
| 16873462 | A model of the mammalian cell-cycle | Regulatory | Metazoan |
| 16968132 | A model of water conservation via stomatal opening in plants | Signaling | Plants |
| 17010384 | A model used to simulate a molecular pathway between two neurotransmitter receptors: dopamine and glutamate receptors | Signaling | Metazoan |
| 17722974 | A model of Tcell activation via the Tcell receptor, the CD4/CD8 co-receptors, and the accessory signaling receptor CD28 | Signaling | Metazoan |
| 18194572 | A logical model of HGF and H. pylori induced c-Met signal transduction | Disease | Metazoan |
| 18433497 | A model of cellular immune response integrating toll-like receptor, interferon, NF-kappaB and apoptotic pathways | Signaling | Metazoan |
| 18463633 | A model of cyclic gene expression during cell division in budding yeast | Regulatory | Primitive |
| 18852469 | A model describing the survival of cytotoxic T lymphocytes in Tcell large granular lymphocyte (T-LGL) leukemia | Disease | Metazoan |
| 19025648 | A model of physiological regulation in cholesterol biosynthesis | Metabolic | Metazoan |
| 19118495 | A regulatory model of the cell-cycle involving the transmembrane tyrosine kinase ERBB2 | Disease | Metazoan |

| | | | |
|---|---|---|---|
| 19144179 | A model of glucose regulation in yeast | Metabolic | Primitive |
| 19185585 | A model of budding yeast cell-cycle | Regulatory | Primitive |
| 19422837 | A model of apoptosis involving external growth factors | Signaling | Metazoan |
| 19524598 | The simplified model of regulation of apoptosis via the NFkB pathway | Biochemical | Metazoan |
| 19622164 | A model of the external signaling molecule TNF$\alpha$ | Disease | Metazoan |
| 19622164 | A model of the external signaling molecule TNF$\beta$1 | Disease | Metazoan |
| 20169167 | A model of the Pseudomonas syringae | Disease | Primitive |
| 20221256 | A model of the interplay between the NFkB pro-survival pathway, RIP1-dependent necrosis, and the apoptosis pathway in response to death receptor-mediated signals | Biochemical | Metazoan |
| 20221256 | A model of apoptosis involving death-receptor mediated signals | Regulatory | Metazoan |
| 20659480 | ABA-induced closure model (ABA signal transduction network) | Signaling | Plants |
| 20862356 | A gene regulatory model of spatial expression patterns in the cerebral cortex | Regulatory | Metazoan |
| 21563979 | A model of glucose regulation via the Lac operon | Metabolic | Primitive |
| 21639591 | A model for phospholipase C-coupled calcium signaling pathways | Signaling | Metazoan |
| 21853041 | A model of myeloid differentiation | Regulatory | Metazoan |
| 21968890 | A model of signaling pathway involving the pro-inflammatory cytokines interleukin 1 (IL-1) | Signaling | Metazoan |
| 21968890 | A model of signaling pathway involving the pro-inflammatory cytokines interleukin 6 (IL-6) | Signaling | Metazoan |
| 22102804 | A model of Tcell large granular lymphocyte (T-LGL) leukemia | Disease | Cancer |
| 22102804 | A reduced model of Tcell large granular lymphocyte (T-LGL) leukemia | Disease | Metazoan |
| 22192526 | A model of the Arabidopsis thaliana root stem cell niche | Signaling | Plants |
| 22253585 | A model of host immune response to single and coin-fection | Disease | Primitive |
| 22253585 | A model of within-host immuno-dynamics | Disease | Primitive |
| 22253585 | A model of host immune response to single and coin-fection | Disease | Primitive |
| 22267503 | A model of Fanconi Anemia/Breast Cancer pathway elucidating the repair of DNA strands | Disease | Metazoan |
| 22448278 | A model of Mycobacterium tuberculosis | Disease | Primitive |
| 22962472 | A model of keratinocyte cell migration mediated by hepatocyte growth factors | Signaling | Metazoan |
| 23049686 | A model of cell-cycle in budding yeast | Regulatory | Primitive |
| 23056457 | A model of gene regulation underlying early cardiac development in mammals | Regulatory | Metazoan |
| 23081726 | A model of the Influenza A virus replication cycle | Disease | Primitive |
| 23134720 | A model linking the oxidative stress pathway to apoptosis | Biochemical | Metazoan |
| 23169817 | A model of the simplified p53 network with high DNA damage | Disease | Cancer |
| 23169817 | A model of the simplified p53 network with low DNA damage | Disease | Cancer |

| | | | |
|---|---|---|---|
| 23171249 | A regulatory model of the TOL multi-protein complex system found on the cell membrane of gram-negative bacteria | Metabolic | Metazoan |
| 23233838 | A signaling pathway model of apoptosis in yeast | Regulatory | Primitive |
| 23469179 | A model of cancer network regulated by miR-17-92 cluster | Disease | Cancer |
| 23520449 | A model of body segmentation in drosophila melanogaster | Biochemical | Metazoan |
| 23743337 | A gene regulatory network model of T lymphocyte differentiation | Regulatory | Metazoan |
| 23764028 | A model of the effect of TGF-$\beta$1 on mosquitos with the parasite Plasmodium falciparum | Disease | Metazoan |
| 23868318 | A model of FGF signaling pathway in drosophila | Regulatory | Metazoan |
| 23868318 | A model of interaction between nine key signaling pathways in drosophila | Regulatory | Metazoan |
| 23868318 | A model of interaction between nine key signaling pathways in drosophila | Regulatory | Metazoan |
| 23868318 | A model of receptor signaling pathways, including EGFR, G-protein-coupled receptor, integrin, and stress pathways | Regulatory | Metazoan |
| 23868318 | A model of receptor signaling pathways, including EGFR, G-protein-coupled receptor, integrin, and stress pathways | Regulatory | Metazoan |
| 23868318 | A model of receptor signaling pathways, including EGFR, G-protein-coupled receptor, integrin, and stress pathways | Regulatory | Metazoan |
| 24069138 | A threshold model of the cell-cycle control network of yeast S. pombe | Regulatory | Primitive |
| 24079299 | A regulatory model of Salmonella typhimurium | Disease | Primitive |
| 24250280 | A comprehensive and generic reaction map for the MAPK signaling network | Disease | Metazoan |
| 24376455 | A model of a metastatic melanoma network | Disease | Cancer |
| 24564942 | A threshold model of the C. elegans early embryonic cell-cycle | Regulatory | Metazoan |
| 24970389 | A protein interaction model to elucidate drug resistance in breast cancer | Disease | Cancer |
| 24970389 | A cell signaling network model to elucidate drug resistance in breast cancer | Disease | Cancer |
| 24970389 | A protein interaction model to elucidate drug resistance in breast cancer | Disease | Cancer |
| 24970389 | A protein interaction model to elucidate drug resistance in breast cancer | Disease | Cancer |
| 24970389 | A protein interaction model to elucidate drug resistance in breast cancer | Disease | Cancer |
| 24970389 | A protein interaction model to elucidate drug resistance in breast cancer | Disease | Cancer |
| 25063553 | A model of the hormonal control of hepatic metabolism using insulin and glucagon signaling | Metabolic | Metazoan |
| 25063553 | A model of the hormonal control of hepatic metabolism using insulin and glucagon signaling | Metabolic | Metazoan |
| 25063553 | A model of the hormonal control of hepatic metabolism using insulin and glucagon signaling | Metabolic | Metazoan |

| | | | |
|---|---|---|---|
| 25063553 | A model of the hormonal control of hepatic metabolism using insulin and glucagon signaling | Metabolic | Metazoan |
| 25163068 | A model of the complete quorum sensing system of Pseudomonas aeruginosa | Signaling | Primitive |
| 25189528 | A model of epithelial-to-mesenchymal transition (EMT) integrating the signaling pathways involved in developmental EMT and known dysregulations in invasive hepatocellular carcinoma (HCC) | Disease | Metazoan |
| 25538703 | A model elucidating the role of the CAV1 scaffold protein in Tcell leukemia | Disease | Metazoan |
| 25780058 | A model of a Rho-family GTPases signaling network | Disease | Metazoan |
| 25908096 | A model of iron acquisition and oxidative stress response in the fungal pathogen aspergillus fumigatus | Metabolic | Primitive |
| 25980672 | A model of the melanogenesis signaling network | Signaling | Metazoan |
| 26090929 | An integrated regulatory and signaling pathway model of the fate of the CD4+ T immune cells | Biochemical | Metazoan |
| 26102287 | A model describing the infection response of Clostridium difficile to antibiotic treatment | Disease | Primitive |
| 26163548 | A signaling pathway model describing the interaction between a drug and cellular outcomes in multiple myeloma cells | Signaling | Metazoan |
| 26207376 | A model of gene regulation in the cardiac progenitor cells involved in early vertebrate development | Regulatory | Metazoan |
| 26244885 | A model of the Septation Initiation Network | Regulatory | Metazoan |
| 26244885 | A model of the Septation Initiation Network that controls cytokinesis in fission yeast | Regulatory | Metazoan |
| 26340681 | A model of cell-cycle regulation in plants | Regulatory | Plants |
| 26346668 | A model is used to map environmental and flow induced signals to endothelial cell phenotype (proliferation, migration, apoptosis, and lumen formation) | Disease | Cancer |
| 26385365 | A model of how mutations in the FA/BRCA pathway cause Fanconi anemia | Disease | Metazoan |
| 26408858 | A model of the regulatory network of lymphopoiesis | Regulatory | Metazoan |
| 26446703 | A model of colitis-associated colon cancer involving P53, MDM2, and AKT | Disease | Metazoan |
| 26528548 | A regulatory network model of early metasis development | Disease | Cancer |
| 26573569 | A regulatory network model of the differentiation of the human gonadal cells into testes or ovaries | Regulatory | Metazoan |
| 26616283 | A model of oncogenic pathways in NB | Disease | Cancer |
| 26751566 | A dynamic model for the regulatory network that controls terminal B cell differentiation | Biochemical | Metazoan |
| 27138333 | A model of the signaling network associated with RCP-driven invasive migration | Disease | Cancer |
| 27148350 | A model linking the nerve growth factor NGF to the proliferation or differentiation outcomes of the cell | Biochemical | Metazoan |
| 27464342 | A model of the M1 (LPS-activated) and M2 (IL-4/13-activated) macrophage polarization types | Signaling | Metazoan |
| 27542373 | A model of the allowed long-term behaviors of the stomatal opening process in plants | Signaling | Plants |
| 27594840 | A model linking the hematopoietic stem progenitor cells and mesenchymal stromal cells in the bone marrow | Disease | Metazoan |

| | | | |
|---|---|---|---|
| 27613445 | A model of the signaling pathways that control S-phase entry and a specific type of senescence called geroconversion | Regulatory | Metazoan |
| 28187161 | A Boolean network CARENET (CAmbium REgulation gene NETwork) for modeling cambium activity | Regulatory | Plants |
| 28209158 | A model of tumorigenic transformation of human epithelial cells | Disease | Cancer |
| 28361666 | A model of castration-resistant prostate cancer | Disease | Cancer |
| 28381275 | A model of colorectal tumorigenesis | Disease | Cancer |
| 28426669 | A model of the gene regulatory network Arabidopsis thaliana | Regulatory | Plants |
| 28426669 | A model of the gene regulatory network Arabidopsis thaliana | Regulatory | Plants |
| 28455685 | A model of the epidermal growth factor receptor signaling of a breast epithelial cell line, MFC10A. | Disease | Cancer |
| 28584084 | A model encompassing the main transcription factors and signaling components involved in myeloid and lymphoid development. | Biochemical | Metazoan |
| 28639170 | A model of the well-known arabinose operon in E. coli | Metabolic | Primitive |
| 29186334 | A model to describe temporal expression patterns observed in GMP-derived cells | Regulatory | Metazoan |
| 29206223 | A model to predict different in-silico knockouts that prevent key SASP-mediators, IL-6 and IL-8, from getting activated upon DNA damage | Biochemical | Metazoan |
| 29230182 | A model of the molecular regulatory network involved in the control of angiogenesis | Biochemical | Metazoan |
| 29237040 | A logical model of initiation of the metastatic process in cancer | Disease | Cancer |
| 29378814 | a model to predict stabilized Pluripotent stem cells (PSC) gene regulatory network (GRN) states in response to input signals | Regulatory | Metazoan |
| 29596489 | A mathematical in silico model that robustly recapitulates the crosstalk between IGF and Wnt signaling. | Signaling | Metazoan |
| 29622038 | A phenotype control kernel (PCK) model of the mitogen-activated protein kinase (MAPK) model | Disease | Metazoan |
| 29632237 | A model used to identify key proteins regulating bortezomib | Disease | Cancer |
| 30024932 | A model of the G2/M checkpoint arrest regulation contemplating the influence of miR-449a | Disease | Metazoan |
| 30038409 | A model of genes/proteins responsible for loss/gain of function in human pluripotent stem cells | Regulatory | Metazoan |
| 30104572 | A model of cell state transition of epithelial-to-mesenchymal transition (EMT) | Disease | Cancer |
| 30116195 | A model of the regulation in the differentiation process of major Tcell subtypes, i.e., Th1, Th2, Th17 and iTreg cells. | Biochemical | Metazoan |
| 30281473 | A model of the aberrant signaling in pancreatic cancer | Disease | Cancer |
| 30323768 | A model gene regulatory network (GRN) of latent proviruses in resting CD4+ Tcell to visualize the complexity of the HIV-1 gene expression | Disease | Metazoan |
| 30518777 | A model of the ABA signaling pathway | Signaling | Plants |

| | | | |
|---|---|---|---|
| 30530226 | A model of the crosstalk between the TGF$\beta$, p38 MAPK and cell-cycle checkpoint pathways which qualitatively describes this dual behavior of TGF-$\beta$ | Signaling | Metazoan |
| 30546316 | A model for the gene regulation driving macrophage polarization to the M1, M2a, M2b, and M2c phenotypes | Signaling | Metazoan |
| 30953496 | A model integrating the insulin resistance pathway with pancreatic $\beta$-cell apoptosis pathway which are responsible for Type 2 diabetes mellitus (T2DM) | Disease | Metazoan |
| 30953496 | A model integrating the insulin resistance pathway with pancreatic $\beta$-cell apoptosis pathway which are responsible for Type 2 diabetes mellitus (T2DM) | Disease | Metazoan |
| 31048917 | A model of Drosophila melanogaster | Regulatory | Metazoan |
| 31130988 | FA-CHKREC (G2 checkpoint and the checkpoint recovery) model, which explores how FA cells might use DDA (DNA damage adaptation) | Disease | Metazoan |
| 31516637 | A model of cellular metabolic flexibility where the inhibitor, Pyruvate, always blocks PDK activity when it is present in the system. | Metabolic | Metazoan |
| 31516637 | A model of cellular metabolic flexibility where the inhibitor, Pyruvate, only blocks PDK activity when at least one of its activators is absent from the system. | Metabolic | Metazoan |
| 31516637 | A model of cellular metabolic flexibility where Acetyl-CoA mediated activation of PDK bypasses Pyruvate mediated inhibition. | Metabolic | Metazoan |
| 31516637 | A model of cellular metabolic flexibility where Fatty Acid mediated activation of PDK bypasses Pyruvate mediated inhibition. | Metabolic | Metazoan |
| 31949240 | A model of renovascular disease (RVD) | Disease | Metazoan |
| 32054948 | A model of the G1/S checkpoint regulation contemplating the regulatory influences of both miR-34a and miR-16 | Disease | Metazoan |
| 32870080 | A model of the lac operon with feedback | Regulatory | Primitive |

# References


[1] Peter L Hammer, I Rosenberg, Sergiu Rudeanu, et al. On the determination of the minima of pseudo-boolean functions. *Studii si Cercetari matematice*, 14:359–364, 1963.

[2] William H Press, Brian P Flannery, Saul A Teukolsky, and William T Vetterling. Numeric recipes in c: the art of scientific computing. *Camb. Univ. Press Camb*, 1992.